The Function of Interdomain Interactions in Controlling Nucleotide Exchange Rates in Transducin*

Ethan P. Marin‡, A. Gopala Krishna‡§, Vincent Archambault‡, Eugene Simuni‡§¶,
Wing-Yee Fu‡§‖, and Thomas P. Sakmar‡§**

From the §Howard Hughes Medical Institute, ‡Laboratory of Molecular Biology and Biochemistry, The Rockefeller University, New York, New York 10021

The intramolecular contacts in heterotrimeric G proteins that determine the rates of basal and receptor-stimulated nucleotide exchange are not fully understood. The α subunit of heterotrimeric G proteins consists of two domains: a Ras-like domain with structural homology to the monomeric G protein Ras and a helical domain comprised of six α-helices. The bound nucleotide lies in a deep cleft between the two domains. Exchange of the bound nucleotide may involve opening of this cleft. Thus interactions between the domains may affect the rate of nucleotide exchange in G proteins. We have tested this hypothesis in the α subunit of the rod cell G protein transducin ($G\alpha_t$). Site-directed mutations were prepared in a series of residues located at the interdomain interface. The proteins were expressed *in vitro* in a reticulocyte lysate system. The rates of basal and rhodopsin-catalyzed nucleotide exchange were determined using a trypsin digestion assay specifically adapted for kinetic measurements. Charge-altering substitutions of two residues at the interdomain interface, Lys^{273} and Lys^{276}, increased basal nucleotide exchange rates modestly (5–10-fold). However, we found no evidence that interactions spanning the two domains in $G\alpha_t$ significantly affected either basal or rhodopsin-catalyzed nucleotide exchange rates. These results suggest that opening of the interdomain cleft is not an energetic barrier to nucleotide exchange in $G\alpha_t$. Experiments with $G\alpha_{i1}$ suggest by comparison that the organization and function of the interdomain region differ among various G protein subtypes.

Transducin (G_t)[1] is the heterotrimeric guanine-nucleotide binding regulatory protein (G protein) of the rod cell. In the GDP-bound state, the α subunit of transducin $(G\alpha_t)$ does not signal. Following exchange of GDP for GTP, which is catalyzed by photoactivated rhodopsin (R*), $G\alpha_t$ signals to its downstream effector. Physiologically, the detection of dim light requires that the basal nucleotide exchange rates of G_t be very low to prevent background noise and that R*-catalyzed exchange be very efficient, to ensure consistent detection and amplification of light signals.

$G\alpha_t$ consists of two domains: a Ras-like domain, which is structurally similar to the monomeric G protein $p21^{ras}$ (Ras), and a helical domain, which is unique to the heterotrimeric G proteins (1). The bound nucleotide lies in a deep cleft between the two domains (Fig. 1*A*). Although the discovery of this arrangement initially prompted speculation that nucleotide exchange would involve opening of the interdomain cleft (1), and that interactions between the domains might affect the rate of nucleotide exchange, the intramolecular contacts in $G\alpha_t$ that determine the rates of nucleotide exchange remain to be elucidated.

There is evidence that structures that do not directly interact with the nucleotide can modulate both the basal and the receptor-catalyzed rates of nucleotide exchange. For example, although the direct contacts between the protein and the nucleotide are virtually the same in closely related subtypes of G protein, the rates of basal nucleotide exchange vary widely. Furthermore, R* tremendously accelerates nucleotide exchange, yet available evidence indicates that it does not directly contact the nucleotide binding site (2).

One of the regions of the G protein hypothesized to control nucleotide release rates without directly contacting the nucleotide is the interdomain interface. The interface is composed of contacts adjacent to the nucleotide and also interactions that are distant from the nucleotide (Fig. 1). These latter interactions involve residues located on the αD-αE loop (amino acid residues 139–147 of $G\alpha_t$) of the helical domain, the Switch III region (residues 227–238), and the αG region (residues 269–277) of the Ras-like domain (Fig. 1*B*). These interactions have been implicated in mediating the lower rate of dissociation of GTPγS relative to GDP in $G\alpha_{i1}$ (3) and in affecting the basal nucleotide exchange rates in $G\alpha_{i1}$ (4) and $G\alpha_s$ (5, 6). Additionally, studies in $G\alpha_s$ have suggested that interdomain interactions are involved in mediating rapid nucleotide exchange catalyzed by the β_2-adrenergic receptor (7, 8).

We have studied the function of several residues of $G\alpha_t$ that are located at the interdomain interface but do not contact the nucleotide. A number of site-directed mutations of these residues were constructed. The well documented difficulties in expressing and purifying recombinant $G\alpha_t$ were overcome by expressing the mutant proteins *in vitro* in a rabbit reticulocyte lysate system. The rates of basal and R*-catalyzed nucleotide

¶ Current address: Harvard College, 2351 Harvard Yard Mail Center, Cambridge, MA 02138.

‖ Current address: Regeneron Pharmaceuticals, 777 Old Saw Mill River Rd., Tarrytown, NY 10591.

** Associate Investigator of the Howard Hughes Medical Institute. To whom correspondence should be addressed: Box 284, Rockefeller University, 1230 York Ave., New York, NY, 10021. Tel.: 212-327-8288; Fax: 212-327-7904; E-mail: sakmar@rockvax.rockefeller.edu.

[1] The abbreviations used are: G_t, transducin; $G\alpha_t$, α subunit of transducin; $G\beta\gamma_t$, $\beta\gamma$ subunits of transducin; DM, *n*-dodecyl-β-D-maltoside; G protein, guanine nucleotide-binding regulatory protein; R*, signaling active state of rhodopsin; Ras, $p21^{ras}$; GTPγS, guanosine 5'-*O*-(thiotriphosphate); TPCK, L-1-tosylamido-2-phenylethyl chloromethyl ketone; PAGE, polyacrylamide gel electrophoresis.

exchange were measured using a trypsin digestion assay specifically adapted for kinetic measurements. Alteration of two conserved lysine residues, Lys^{273} and Lys^{276}, increased the rate of spontaneous nucleotide exchange 5–10-fold. However, in contrast to what would be predicted based on published structural and biochemical studies, we found no evidence that interactions that span the domain interface were important in either maintaining the low rate of basal nucleotide exchange or in supporting the high rate of R*-catalyzed exchange in $G\alpha_t$. Experiments with $G\alpha_{i1}$ demonstrated that conserved lysine residues serve different roles in $G\alpha_{i1}$ than in $G\alpha_t$. In general, the function of the interdomain region appears to differ among various G protein subtypes.

EXPERIMENTAL PROCEDURES

Reagents—Buffers, nucleotides, protease inhibitors, and salts were from Sigma or Roche Molecular Biochemicals. [^{35}S]Methionine was purchased from PerkinElmer Life Sciences. TPCK-treated trypsin was from Worthington Biochemicals. Synthetic oligonucleotides were purchased from Genelink, Inc. DNA sequencing was carried out using BigDye Terminator Cycle sequencing in the DNA sequencing core facility at the Rockefeller University.

Site-directed Mutagenesis of $G\alpha_t$ and $G\alpha_{i1}$—The parent for all $G\alpha_t$ constructs was pGEM2sTα, the synthetic bovine $G\alpha_t$ gene (9) cloned into the pGEM2 plasmid under control of a SP6 promoter. Site-directed point mutations were prepared using the QuikChange method (Stratagene). For each mutant, two complementary primers were designed that coded for the desired mutation as well as 10–15 bases of complementary sequence on either side of the mutation site. Most amino acid substitutions could be accomplished with two or less nucleotide changes. The total length of each primer was 20–30 bases. The mutagenesis reaction (50 μl final) consisted of 5 ng of template plasmid, 1 μl of cloned *Pfu* polymerase (2.5 units/μl) (Stratagene), 5 μl of 10× *Pfu* buffer (Stratagene), 250 nM concentration of each primer, 800 μM concentration dNTP mix. The reactions were thermocycled in a GeneAmp 9600 (PerkinElmer Life Sciences) thermocycler with the following program: 3 min at 95 °C, 14 cycles of 30 s at 95 °C, 1 min at 55 °C, 8 min at 68 °C, and then 10 min at 72 °C. Amplification of the mutated plasmid was verified by running 1 μl of the reaction on a 1% agarose gel. The parental plasmid was selectively digested using the restriction enzyme *Dpn*I (New England Biolabs) for 1.5 h at 37 °C. Since *Dpn*I digests only methylated DNA, the wild-type template plasmid was restricted. The *Dpn*I-treated mutant plasmid was transformed into chemically competent bacteria (subcloning efficiency DH-5α (Life Technologies, Inc.) or OneShot TOP10 (Invitrogen)). Generally the ratio of recombinant transformants following transformations with QuikChange reactions done with primers compared with control reactions run without primers was >50:1. All constructs were verified by automated DNA sequencing of the entire coding region of $G\alpha_t$.

The parent for all $G\alpha_{i1}$ constructs was pGEM2Gα_{i1}, the $G\alpha_{i1}$ gene cloned into the pGEM2 plasmid under control of a SP6 promoter. To improve expression, a 217-base pair segment of the 5′-untranslated region was removed by QuikChange mutagenesis.

Transcription and Translation of $G\alpha_t$ in Vitro—Recombinant $G\alpha_t$ subunits were prepared using the TNT Quick Coupled rabbit reticulocyte lysate transcription/translation kit (Promega). For each translation, 20 μl of lysate mix was combined with 4 μl of DNA (0.5 μg total) and 1 μl of ~9 μM [^{35}S]methionine (PerkinElmer Life Sciences) at a specific activity of approximately ~1250 Ci/mmol. The reactions were incubated at 30 °C for 90 min. Subsequent manipulations were performed on ice or at 4 °C. The translated products were passed over BioSpin 6 gel filtration spin columns (Bio-Rad) twice consecutively to remove excess nucleotides and [^{35}S]methionine. The volume of each reaction was then adjusted to 100 μl in Buffer A (5 mM Tris-HCl, pH 7.5, 150 mM NaCl, 2 mM MgCl$_2$, 1 mM dithiothreitol, 0.01% (w/v) *n*-dodecyl-β-D-maltoside (DM)). If the reaction was to be studied in a R*-catalyzed assay, G$\beta\gamma_t$ was added to a final concentration of 30 nM. Every experiment was performed using freshly translated material.

Trypsin Proteolysis and Analysis—The digestion procedure was adapted from Garcia *et al.* (10). Aliquots (8 μl) of the reaction mix were withdrawn and mixed with 1.5 μl of digest buffer (5% Lubrol, 2 mM GDP, 1 mg/ml TPCK trypsin) or digest control buffer (5% Lubrol, 2 mM GDP). The digests were incubated on ice for 30 min ($G\alpha_t$ samples) or for 5 min ($G\alpha_{i1}$ samples). Digestion was terminated by the addition of 2.5 μl of termination solution (10 mg/ml aprotinin, 10 μM phenylmethylsulfonyl fluoride), followed by 6 μl of 3× SDS sample buffer (New England

Biolabs). Samples were frequently stored at −20° for up to 48 h. Subsequently, the samples were boiled for 3 min, and the protein fragments were resolved by SDS-PAGE on 15% pre-cast Tris-HCl minigels (Bio-Rad). Following electrophoresis, the gels were fixed for >30 min in 50% MeOH/10% acetic acid and then soaked for 5 min in 7% methanol/7% acetic acid/2% glycerol. The gels were vacuum-dried onto filter paper (Whatman), and the radiolabeled $G\alpha_t$ bands were visualized by exposing the gels to a storage phosphor screen (Molecular Dynamics) for 1–7 days.

Data Analysis of Trypsin Proteolysis Patterns—The phosphor storage screens were scanned using a Storm Imager machine (Molecular Dynamics) at 200-micron resolution. The resulting images of the gels were analyzed using ImageQuant software (Molecular Dynamics). Lines were drawn down the center of each lane on the gel image, perpendicular to the bands. The intensity of each pixel along the line was determined as the average of 5–10 pixels on either side of the line. In this way, most of the width of each lane was considered. Any defect in the gel was avoided by careful placement of the lines. The intensity of each pixel was plotted as a function of position along the line so that the bands on the gel were represented as peaks on the graph. The base line of the graph was set so as to exclude nonspecific background intensity. GDP-bound $G\alpha_t$ yielded a ~23-kDa band, whereas GTPγS-bound or GDP/AlF$_4^-$-bound $G\alpha_t$ yielded a ~34-kDa band. The areas of the peaks corresponding to the ~23- and ~34-kDa bands were then calculated and recorded in an Excel spreadsheet. The fraction of functional $G\alpha_t$ in the GTPγS-bound state in a given lane was determined by the following formula: (area of ~34-kDa peak)/((1.4 × area of ~23-kDa peak) + (area of ~34-kDa peak)). The area of the ~23-kDa peak was multiplied by 1.4 to normalize for the smaller number of methionines in the smaller fragment relative to those in the ~34-kDa fragment. This coefficient was adjusted (to 1.3) for analysis of samples in which Met^{228} was replaced. Activation kinetics were analyzed by plotting the fraction of $G\alpha_t$ activated as a function of time. In the basal exchange rate assays, the data were fit to a single exponential rise to a maximum equation of the form: percent activated $= c + 100(1 - \exp(-kt))$. The apparent rate constants derived from the fits are presented in Table I.

For experiments conducted with $G\alpha_{i1}$, the intensity of the GDP-dependent band could not be determined reliably due to nonspecific background intensities in the region of the gel where the GDP band migrated. This background was present even in undigested samples of $G\alpha_{i1}$. Since the ratio of the GTPγS-dependent band to the sum of the GTPγS and GDP bands could not be determined, the intensity of the GTPγS band was expressed as a fraction of the total intensity in each lane. Activation time courses were plotted as the change in this intensity over time. For fully activated $G\alpha_{i1}$, the GTPγS band accounted for roughly 25–30% of the intensity in the lane.

Control Reactions for Trypsin Proteolysis of $G\alpha_t$—Control reactions were performed on each sample to check the quantity and apparent molecular mass of the expressed protein, as well as the digest patterns following incubation with GDP and GDP/AlF$_4^-$. From each 100-μl sample of translated $G\alpha_t$, 30 μl was removed and combined with 100 μM GDP. Of this 30 μl, one 8-μl aliquot was digested ("+GDP"); another 8-μl aliquot was mock-digested with digest control buffer ("undigested"). The remaining 14 μl was combined with a final concentration of 0.17 mM AlCl$_3$ and 10 mM NaF added from separate 30× stock solutions. Following a 10-min incubation at room temperature, an 8-μl aliquot was removed and digested ("+GDP/AlF$_4^-$").

Basal Nucleotide Exchange Time Course of $G\alpha_t$—Samples (70 μl each) of translated $G\alpha_t$ or mutant $G\alpha_t$ in Buffer A were quickly warmed to room temperature in a water bath, and GTPγS was added to a final concentration of 100 μM. Aliquots (8 μl) were withdrawn at 1, 2, 3, 4, and 6 h following GTPγS addition and digested. The activity of the protein following 6-h incubation at room temperature was investigated by addition of R* and G$\beta\gamma_t$ (30 nM each, see below) and incubation under room light for 20 min. A final 8-μl aliquot was then removed and digested. For $G\alpha_{i1}$ samples, which activated very quickly, aliquots were taken for a 180-min time course, and the R*/G$\beta\gamma_t$ mix was not added.

R/G$\beta\gamma_t$-catalyzed Activation Time Course of $G\alpha_t$*—Samples (70 μl each) of translated $G\alpha_t$ or mutant $G\alpha_t$ in Buffer A were quickly warmed to room temperature in a water bath. A mixture of R* and GTPγS (4 μl) was added to the sample yielding a final concentration of 30 nM R* and 14 μM GTPγS. Immediately before addition to the reaction, the rhodopsin was photolyzed by illumination for 15 s with a fiber optic cable connected to a Dolan Jenner lamp equipped with a >495-nm long-pass filter. The samples were incubated at room temperature under illumination. Aliquots (8 μl) were withdrawn and digested at 1, 2, 3, 5, 10, and 20 min following addition of the R*/GTPγS mix.

Preparation of G_t, $G\alpha_t$, $G\beta\gamma_t$, and Rhodopsin from Bovine Reti-

TABLE I
Rate constants for basal nucleotide exchange measured for $G\alpha_t$ and $G\alpha_t$ mutants

Arranged by amino acid position			Arranged by basal exchange rate		
Mutant	k_{app}[a]	-Fold increase[b]	Mutant	k_{app}[a]	-Fold increase[b]
Wild-type	8.6 ± 0.7	1.0 ± 0.1	D227N	3.4 ± 0.6	0.4 ± 0.1
S140A	14.7 ± 4.6	1.7 ± 0.6	M228L	4.0 ± 0.4	0.5 ± 0.1
S140N	7.8 ± 2.1	0.9 ± 0.3	V231A	4.6 ± 0.6	0.5 ± 0.1
S140R	12.1 ± 2.6	1.4 ± 0.3	D227A	5.0 ± 1.1	0.6 ± 1.1
Q143A	6.1 ± 1.4	0.7 ± 0.2	Q143A	6.1 ± 1.4	0.7 ± 0.2
D227A	5.0 ± 1.1	0.6 ± 1.1	M228Q	6.2 ± 0.6	0.7 ± 0.1
D227N	3.4 ± 0.6	0.4 ± 0.1	V231W	6.4 ± 1.1	0.7 ± 0.1
M228A	14.6 ± 0.7	1.7 ± 0.2	S140A/D227N	7.4 ± 0.7	0.9 ± 0.1
M228L	4.0 ± 0.4	0.5 ± 0.1	S140N	7.8 ± 2.1	0.9 ± 0.3
M228Q	6.2 ± 0.6	0.7 ± 0.1	Wild-type	8.6 ± 0.7	1.0 ± 0.1
V231A	4.6 ± 0.6	0.5 ± 0.1	K276R	8.8 ± 2.5	1.0 ± 0.3
V231W	6.4 ± 1.1	0.7 ± 0.1	S140A/Q143A	10.4 ± 4.7	1.2 ± 0.3
K273A	39.0 ± 22.6	4.6 ± 2.7	K275A	12.0 ± 1.4	1.4 ± 0.6
K275A	12.0 ± 1.4	1.4 ± 0.2	S140R	12.1 ± 2.6	1.4 ± 0.2
K276A	45.1 ± 7.5	5.3 ± 1.0	D227N/K273A	14.5 ± 2.7	1.7 ± 0.3
K276E	98.8 ± 29.1	11.5 ± 3.5	M228A	14.6 ± 0.7	1.7 ± 0.3
K276R	8.8 ± 2.5	1.0 ± 0.3	S140A	14.7 ± 4.6	1.7 ± 0.2
S140A/Q143A	10.4 ± 4.7	1.2 ± 0.6	D227A/K276A	14.8 ± 7.3	1.7 ± 0.9
S140A/K276A	67.3 ± 14.0	7.9 ± 1.8	D227N/K276A	20.3 ± 4.7	2.4 ± 0.6
S140A/D227N	7.4 ± 0.7	0.9 ± 0.1	K273A	39.0 ± 22.6	4.6 ± 2.7
S140R/K276A	48.0 ± 14.6	5.6 ± 1.8	K276A	45.1 ± 7.5	5.3 ± 1.0
D227A/K276A	14.8 ± 7.3	1.7 ± 0.9	S140R/K276A	48.0 ± 14.6	5.6 ± 1.8
D227N/K273A	14.5 ± 2.7	1.7 ± 0.3	S140A/K276A	67.3 ± 14.0	7.9 ± 1.8
D227N/K276A	20.3 ± 4.7	2.4 ± 0.6	K276E	98.8 ± 29.1	11.5 ± 3.5

[a] The apparent rate constants were derived from fits of each data set to the exponential rise equation, $y = c + 100(1 - \exp(-kt))$. Each mutant was assayed at least three times (WT $G\alpha_t$ was assayed 26 times), and an independent fit was made to each data set. The values reported are the mean $k_{app} \times 10^4$ min^{-1} ± 2 × S.E. The catalyzed activation rate of wild-type $G\alpha_t$ was determined to be 5390 ± 802 in the presence of 30 nM photoactivated rhodopsin, 30 nM $G\beta\gamma_t$, and 14 μM GTPγS. This is a 629 ± 107-fold increase over the basal (uncatalyzed) rate.
[b] The -fold increase in the rate of the mutant relative to that of wild-type is calculated at the k_{app}(mutant)/k_{app}(wild-type).

nas—G_t was prepared from frozen bovine retinas (Lawson, Inc., Lincoln, NE) using standard techniques (11, 12) as described previously (13). $G\beta\gamma_t$ and $G\alpha_t$ were isolated from holo-G_t as described previously (13) using a Hitachi LC-organizer high performance liquid chromatography system with a 1-ml Hi-Trap Blue-Sepharose column (Amersham Pharmacia Biotech). The proteins were eluted from the column by applying a 0–2 M NaCl gradient. $G\beta\gamma_t$ concentrations were determined using the Bio-Rad protein assay reagent according to manufacturer's instructions. Concentrations of G_t and $G\alpha_t$ samples were determined by spectrofluorometric titration as described previously (14). The proteins were stored at −20 °C in a 50% glycerol buffer until use. Purified recombinant $G\alpha_{i1}$ expressed in *Sf*9 cells was provided by Dr. S. Graber (West Virginia University) (15). Urea-washed disc membranes, the gift of Dr. K. C. Min, were prepared as described elsewhere (16). The membranes were solubilized in 1% DM, and insoluble material was removed by centrifugation. The resulting solubilized rhodopsin displayed a A_{280}/A_{500} spectral ratio of <1.8 and a concentration of ~8 μM.

Fluorescence Activation Traces of $G\alpha_t$ and $G\alpha_{i1}$—The assay was performed essentially as described previously (14) using a Spex Fluorolog spectrofluorometer equipped with a 150-watt xenon arc lamp. A solution of 250 nM concentration of $G\alpha_t$ or $G\alpha_{i1}$ was prepared in fluorescence buffer (100 mM NaCl, 10 mM Tris-HCl, pH 6.9, 2 mM MgCl$_2$, 1 mM dithiothreitol, 0.01% (w/v) DM). Solution (0.5 ml) was placed in a quartz microcuvette and loaded into the thermojacketed cuvette holder equipped with a magnetic stirrer at 25 °C. Protein fluorescence was excited at 300 nm with 2-nm slit width, and emission intensity was collected at 345 nm with a 12-nm slit width. The activation reaction was initiated by injecting 15 μl of GTPγS solution to a final concentration of 5 μM. Nucleotide exchange was observed as an increase in the intensity of tryptophan fluorescence emission that results from conformational changes in Trp^{207} that occur upon binding GTP (17).

RESULTS

A series of site-directed mutants of $G\alpha_t$ with replacements of residues located at the interdomain interface was prepared. Sites were selected for mutation based on their position in the crystal structure of GDP-bound $G\alpha_t$ (18) (Fig. 1), as well as their importance in $G\alpha_{i1}$ and $G\alpha_s$ suggested by published studies (see below). Selected residues were replaced with alanine, or with the amino acid present in the homologous position of either $G\alpha_{i1}$ or $G\alpha_s$, and/or with amino acids reported to cause

altered phenotypes in $G\alpha_{i1}$ or $G\alpha_s$. For each mutant $G\alpha_t$, the rates of both basal (*i.e.* uncatalyzed) and R*-catalyzed nucleotide exchange were measured.

Expression of $G\alpha_t$ in Vitro and Trypsin Digestion Assay of Nucleotide Binding and Exchange—All $G\alpha_t$ constructs were expressed *in vitro* in a coupled transcription/translation rabbit reticulocyte lysate system. Time course experiments confirmed that *in vitro* expression was maximal in 90 min (not shown). Typical reactions with plasmids encoding $G\alpha_t$ or $G\alpha_t$ mutant genes yielded one major protein band at the expected molecular mass of ~40-kDa (Fig. 2). Generally 80–90% of the total intensity in the lane was in the one band. Expressed $G\alpha_t$ was digested with trypsin following various treatments. Inactive, GDP-bound $G\alpha_t$ was prepared by incubating *in vitro* translated $G\alpha_t$ with 100 μM GDP. Trypsin proteolysis of this sample resulted in the formation of a ~23-kDa fragment (Fig. 2). The active conformation was prepared by incubating $G\alpha_t$ with GDP and AlF$_4^-$. AlF$_4^-$ is known to bind to Gαt-GDP and simulate the presence of the γ-phosphate of GTP. Therefore, a conformation nearly identical to the activated GTP-bound conformation is induced (19). Digestion of the AlF$_4^-$-activated Gαt yielded a ~34-kDa band and no ~23-kDa band. Similarly, activation of $G\alpha_t$ with GTPγS yielded an identical ~34-kDa band following trypsin digestion (Fig. 2).

In all cases, trypsin proteolysis produced a variety of lower molecular weight fragments. Some of these were the smaller polypeptides that were cleaved to produced the ~23- and ~34-kDa fragments. Others likely resulted from extensive proteolysis of protein that was not properly folded. This is consistent with the large number of potential trypsin sites present in the primary structure of $G\alpha_t$ and the relatively small number of accessible sites in the properly folded tertiary structure. The fraction of the total pool of translated $G\alpha_t$ that was properly folded and functional was estimated from the ratio of the intensities of the ~34-kDa band following GDP/AlF$_4^-$ treatment (*i.e.* the properly folded, activable pool) to that of the ~40-kDa
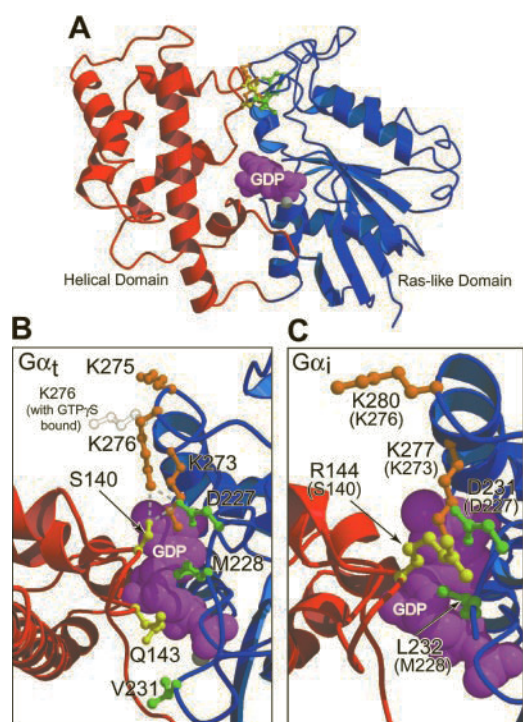
FIG. 1. **Crystal structures of the interdomain interface of GDP-bound $G\alpha_t$ (Protein Data Bank number 1tag) and $G\alpha_{i1}$ (Protein Data Bank number 1gdd).** Side chains of residues that have been mutated in this study are shown in *ball-and-stick* representation. Side chains of residues in the helical domain are *yellow*, those from Switch III are *green*, and those from the αG region are *orange*. The figures were prepared with Molscript (32) and Raster3D (33). *A*, overall view of the $G\alpha_t$ protein. The Ras-like domain is *blue*, the helical domain is *red*, and the GDP is *purple*. The nucleotide resides in a cleft between the two domains. The side chains of many of the residues studied in this report potentially interact with each other across the interdomain interface, but do not directly contact the nucleotide. *B*, the protein has been rotated 90° about the horizontal axis relative to *A*, and the interdomain region is enlarged. Hydrogen bonds are shown as *dotted lines*. The position of Lys[276] in the GTPγS-bound $G\alpha_t$ structure is shown as an *outline*. *C*, the structure of GDP-bound $G\alpha_{i1}$ from a similar viewpoint as in *B*. The corresponding amino acid number in $G\alpha_t$ is given in *parentheses*.

band in the undigested sample (*i.e.* the total pool of translated full-length protein). This ratio was generally about 0.15 for wild-type $G\alpha_t$ and severalfold higher for $G\alpha_{i1}$. This result parallels the functional expression levels of $G\alpha_t$ and $G\alpha_{i1}$ that have been observed in other heterologous expression systems. Thus, *in vitro* expression might serve as a rapid and useful predictor of the expression level of a given G protein construct in other systems.

The rate of trypsin proteolysis of GDP- and GDP/AlF$_4^-$-treated $G\alpha t$ and the stabilities of the resulting fragments were investigated by digestion time course experiments. Both the ~23- and ~34-kDa bands formed completely by 20 min and remained stable until at least 40 min in the presence of trypsin (data not shown). We therefore chose to stop the digestion after 30 min in all experiments. Similar experiments with $G\alpha_{i1}$ indicated that digestion occurred more quickly. Accordingly, digests were run for 5 min with $G\alpha_{i1}$ samples.

Three major sites of trypsin proteolysis in properly folded $G\alpha_t$ have been identified: Lys[18], Arg[204], and Arg[310] (20). Using site-directed mutagenesis, we investigated which of these sites were contributing to the fragments produced under the digestion conditions used in this study. The mutants K18A, R204H, and R310A were prepared, expressed *in vitro*, and digested following treatment with either GDP or GDP/AlF$_4^-$.

Formation of the ~23-kDa band following treatment with GDP was altered only by the R204H mutation (not shown).
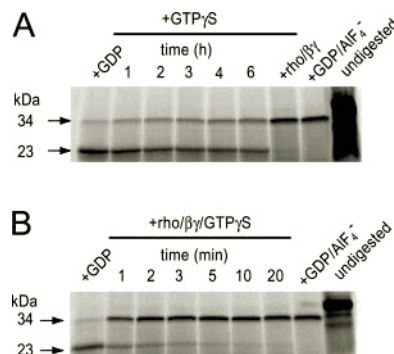

FIG. 2. **Determination of nucleotide exchange rates by analysis of trypsin digestion patterns.** $G\alpha_t$ was expressed *in vitro* in a rabbit reticulocyte lysate system and metabolically labeled with [^{35}S]methionine. Translated material was passed twice over gel filtration spin columns to remove free nucleotides and then treated with various conditions as indicated. Aliquots were removed and digested with trypsin for 30 min on ice, except where indicated otherwise. The resulting fragments were analyzed by SDS-PAGE and visualized by phosphorimaging. *A*, basal nucleotide exchange. Translated $G\alpha_t$ was mixed with 100 μM GTPγS. Aliquots were removed and digested at 1, 2, 3, 4, and 6 h. Following collection of the 6-h aliquot, R* and $G\beta\gamma$ were added to a final concentration of 30 nM each. After a 20-min incubation, an aliquot was removed and digested (+$rho/\beta\gamma$). Control reactions show undigested $G\alpha_t$ and $G\alpha_t$ digested following incubation with 100 μM GDP or GDP/AlF$_4^-$. *B*, R*/$G\beta\gamma$t-catalyzed nucleotide exchange. Translated $G\alpha_t$ was mixed with 30 nM R*, 30 nM $G\beta\gamma_t$, and 14 μM GTPγS. Aliquots were removed and digested at 1, 2, 3, 5, 10, and 20 min. Control reactions were performed as in *A*.

Arg[204] is the site at which cleavage occurred in the GDP form to yield the ~23-kDa fragment, but which was protected from digestion in the GTPγS-bound conformation. Arg[204] is located in the Switch II region of $G\alpha t$, and crystal structures confirm that it moves from a surface exposed to a buried position upon activation (1, 18). Formation of the ~34-kDa band following activation with GDP/AlF$_4^-$ was affected only by the R310A mutation (not shown). Thus Arg[310] appears to be the site at which trypsin proteolysis occurred to yield the ~34-kDa fragment. The K18A mutant was indistinguishable from wild-type; digestion at Lys[18] does not appear to contribute to the formation of either fragment under the conditions used (not shown). Using these results, the ratio of the number of methionines in the ~34-kDa band relative to the ~23-kDa band was determined to be 1.4. This factor was used to normalize the intensity of the ~23-kDa band in calculating the fraction of activated $G\alpha t$ in each aliquot.

The fraction of $G\alpha_t$ in the active conformation in a partially activated sample was calculated as the intensity of the ~34-kDa band (*i.e.* the activated $G\alpha_t$) divided by the sum of the intensities of the ~23- and ~34-kDa bands. The sum of the intensities of the ~23- and ~34-kDa bands is indicative of the total pool of functional $G\alpha_t$ in the sample. This calculation is therefore internally normalized to the total amount of functional $G\alpha_t$ in each aliquot and does not require comparison with the ~34-kDa band of a separate sample (such as one in a completely activated lane).

The rate of nucleotide exchange of each sample was determined by monitoring the fraction of $G\alpha_t$ in the active conformation at specific times following addition of GTPγS. In the basal exchange rate assay, $G\alpha_t$ was 31% activated at 6 h following GTPγS addition (Fig. 2*A*). The activity of $G\alpha_t$ following the 6-h incubation was confirmed by demonstrating that addition of rhodopsin and $G\beta\gamma_t$ could fully activate the remaining $G\alpha_t$ (Fig. 2). In comparison, $G\alpha_t$ A322S (a mutant known to display high nucleotide exchange rates in $G\alpha_{i1}$ (21) and $G\alpha_s$

FIG. 3. **Basal nucleotide exchange time courses of $G\alpha_t$ and $G\alpha_t$ mutants.** The percent activation at each time point was determined by analysis of trypsin digestion patterns as described under "Experimental Procedures." The time 0 data point is calculated from protein mixed with 100 μM GDP for 10 min. Each data point is the average of three to five independent experiments; wild-type $G\alpha_t$ was assayed 26 times. *Error bars* depict $\pm 2 \times$ S.E. The *solid lines* represent fits to a one-component exponential rise function. *A*, mutations of residues located on the helical domain. *B* and *C*, mutations of residues located on Switch III. *D*, mutations of residues located in the αG region.
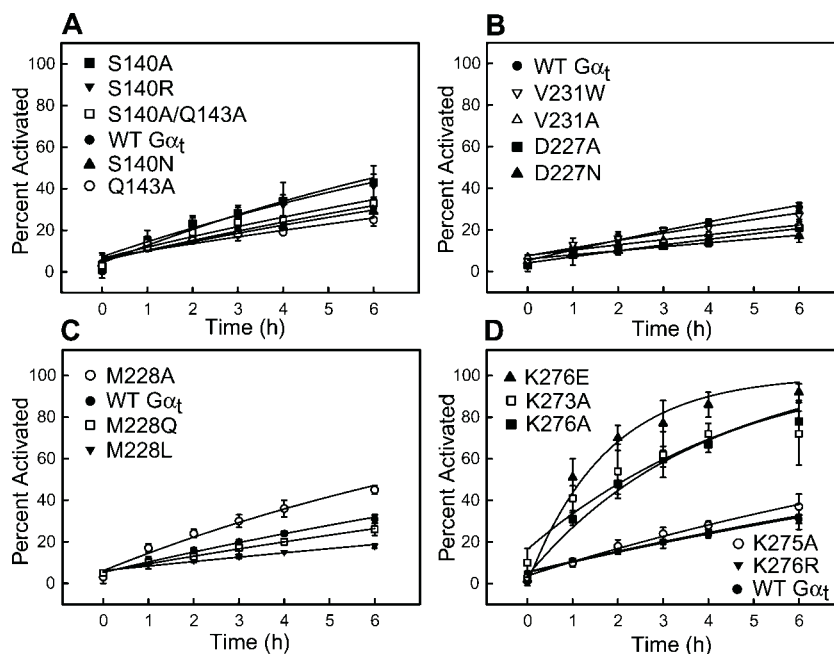
(22)) was 100% activated in less than 1 h.[2]

In R*-catalyzed assays, $G\alpha_t$ was nearly 100% activated in 20 min (Fig. 2*B*). Under the conditions of the assay, the rate of $G\alpha_t$ activation was found to be dependent on the concentration of rhodopsin from 0–100 nM and sensitive to the presence of added $G\beta\gamma_t$ (not shown). Some residual activation was observed in the absence of added $G\beta\gamma_t$, probably as a result of small quantities of $G\beta\gamma$ present in the reticulocyte lysate or the rhodopsin preparations. No rhodopsin-catalyzed activation was observed in the dark (data not shown). Additionally, mutant G348P, which was previously reported to be unable to bind rhodopsin (23), was not activated by R* in this assay (not shown). To our knowledge, this is the first report in which trypsin proteolysis of *in vitro* translated $G\alpha_t$ has been used to measure the kinetics of R*-catalyzed nucleotide exchange.

Analysis of Single Amino Acid Replacements in the Interdomain Interface of $G\alpha_t$—Two residues in the helical domain, Ser[140] and Gln[143], extend toward and interact with residues from the Ras-like domain. Ser[140] was replaced with alanine, arginine (the homologous residue in $G\alpha_{i1}$), and asparagine (the homologous residue in $G\alpha_s$). Gln[143] was mutated to alanine and was also combined with S140A in a S140A/Q143A double mutant. None of these mutations substantially altered the rate of basal (Fig. 3*A*, Table I) or R*-catalyzed nucleotide exchange (not shown).

Several residues in the Switch III region of $G\alpha_t$ were altered by site-directed mutagenesis. The crystal structure suggests that Asp[227] participates in hydrogen bonds with both Ser[140] and Lys[276] (Fig. 1). This residue was replaced with both asparagine (the homologous residue in $G\alpha_s$) and with alanine. The adjacent Met[228] was replaced with alanine, leucine (the equivalent in $G\alpha_{i1}$), and glutamine (the equivalent of a mutation in $G\alpha_{i1}$ reported to increase the GDP release rate (4)). Val[231] was replaced with alanine and with tryptophan. The V231W mutant was prepared to simulate a naturally occurring mutation in the homologous residue of $G\alpha_s$, Arg[258], which was found in a patient with Albright's hereditary osteodystrophy (5). None of these mutations was found to substantially alter either the basal (Fig. 3, *B* and *C*, and Table I) or the R*-catalyzed activation rates (not shown). However, several mutations caused

slight ($\sim$2-fold), but reproducible reductions in the basal nucleotide exchange rate. These mutations include D227A, D227N, V231A, and M228L (Table I).

Three lysine residues in the αG region of $G\alpha_t$ were studied. Lys[273] and Lys[276] are oriented toward Asp[227] of Switch III (Fig. 1). In addition, the crystal structure of $G\alpha_t$-GDP indicates that Lys[276] forms hydrogen bonds with Ser[140] of the helical domain (Fig. 1). Lys[275] extends out toward the solvent (Fig. 1). Lys[273], Lys[275], and Lys[276] were each replaced with alanine. In addition, Lys[276] was replaced with glutamic acid and with arginine. The K273A, K276A, and K276E mutations all resulted in significantly increased rates of basal nucleotide exchange, from 5–10-fold above wild-type (Fig. 3*D*). The K276R mutation did not affect nucleotide exchange rates, nor did mutation of Lys[275]. None of the mutations substantially altered the rate of R*-catalyzed nucleotide exchange (not shown).

Analysis of Double Amino Acid Replacements—To probe for functional interactions between pairs of residues, a series of double amino acid replacements was prepared by site-directed mutagenesis (Table I). The K276A/D227N, K276A/D227A, and K273A/D227N double replacements all displayed slower basal rates of nucleotide exchange than the corresponding single replacements of Lys[276] or Lys[273] (Fig. 4). The double mutants displayed faster exchange kinetics than wild-type $G\alpha_t$, however. Combining amino acid replacements at positions Lys[276] and Ser[140] revealed that the effects on basal exchange rates of each individual mutation were roughly additive (Fig. 4). A combination of amino acid replacements at positions 140 and 227, S140A/D227N, had similar exchange kinetics to that of wild-type $G\alpha_t$ (Table I).

Analysis of $G\alpha_{i1}$ Mutants—$G\alpha_{i1}$ is 66% identical to $G\alpha_t$ at the primary structure level and very similar at the tertiary structure level (Fig. 1*C*). However, the basal nucleotide exchange rate of $G\alpha_{i1}$ has been reported to be significantly higher than that of $G\alpha_t$ (24). We confirmed this observation in studies with recombinant $G\alpha_{i1}$ and retinal $G\alpha_t$ in a fluorescence activation assay (Fig. 5*A*). The rate of basal nucleotide exchange as monitored by increases in fluorescence was much greater in $G\alpha_{i1}$ than in $G\alpha_t$ at 25 °C. However, the rate and the magnitude of fluorescence change were comparable when each protein was fully activated with excess AlF_4^-.

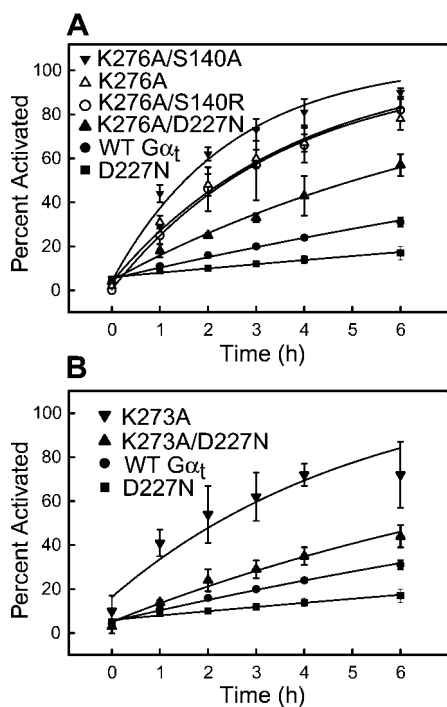$G\alpha_{i1}$ was expressed *in vitro* and studied by trypsin digestion.

FIG. 4. **Time courses of basal nucleotide exchange of double amino acid replacement mutants in Gα_t.** The experiments were conducted as described in the legends to Figs. 2 and 3. *A*, the K276A replacement was combined with mutations of residues that are indicated in the crystal structure to interact with Lys[276]. The basal nucleotide exchange rates were determined. Data for K276A and D227N are replotted from Fig. 3 for comparison with the double mutants. *B*, the K273A mutation was combined with the D227N mutation and the basal activation rate determined. Data for K273A and D227N are re-plotted from Fig. 3 for comparison.

SDS-PAGE analysis indicated that a ~38-kDa band was produced following full activation with either GTPγS or GDP/AlF$_4^-$ and that a smaller fragment resulted from digestion in the presence of GDP. The intensity of the smaller GDP-dependent band of Gα_{i1} could not be accurately quantitated due to reproducible nonspecific background in that portion of the gel. Therefore, the method for determining the fraction of *in vitro* translated Gα_{i1} activated in an aliquot was modified from the "ratio" method used for Gα_t. In each aliquot, the intensity of the ~38-kDa band was determined as a fraction of the total intensity in the lane, and the time course of activation was plotted as a change in this fraction over time (Fig. 5*B*). This analysis suggests that basal nucleotide exchange of GDP for GTPγS by Gα_{i1} was complete in 1 h, significantly faster than that by Gα_t, which was only 32% complete in 6 h. The $t_{1/2}$ for activation of Gα_{i1} (~20 min) was comparable in both the fluorescence and the trypsin protection assays (Fig. 5).

A series of site-directed mutants was prepared in Gα_{i1} to probe for similarities between the functions of interdomain residues in Gα_{i1} and Gα_t. The equivalent of Lys[273] and Lys[276] of Gα_t are conserved in Gα_{i1} as Lys[277] and Lys[280], respectively (Fig. 1). Both were replaced with alanine, expressed *in vitro*, and the basal nucleotide exchange rates of the resulting mutants were determined. Neither of these mutations (K277A and K280A) increased the basal activation rate of Gα_{i1} appreciably (Fig. 5*B*). Additionally Arg[144] of Gα_{i1}, the homolog of Ser[140] in Gα_t, was replaced with serine. Since the Ser[140] of Gα_t forms hydrogen bonds with Lys[276], it was hypothesized that in Gα_{i1} the replacement of Arg[144] with serine might alter the position of Lys[280] (Lys[276] in Gα_t) to resemble the Gα_t conformation and lower the basal rate of nucleotide exchange. However, the opposite was observed. The Gα_{i1} R144S mutant exhibited accel-
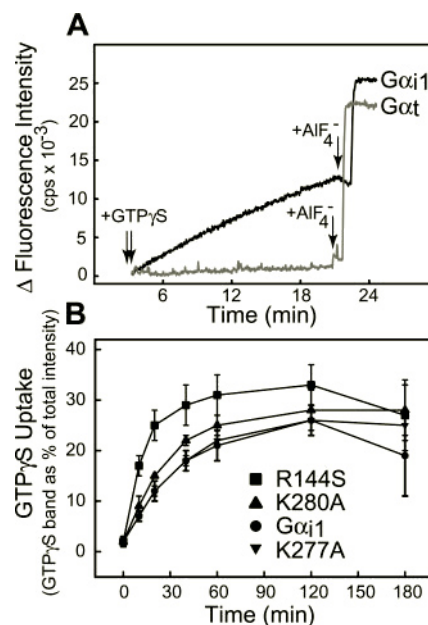

FIG. 5. **Basal nucleotide exchange time course of Gα_{i1} and mutants of Gα_{i1}.** *A*, fluorescence activation traces of Gα_{i1} (expressed and purified from *Sf*9 cells) and Gα_t (purified from bovine retinas) are superimposed. Fluorescence intensity change is plotted as a function of time. At 200 s, GTPγS was added to the cuvette to start the reaction. At the times indicated by the *arrows*, AlCl$_3$ and NaF were added from separate stock solutions to form AlF$_4^-$. *B*, basal nucleotide exchange rates of Gα_{i1} and mutants expressed *in vitro* and assayed by analysis of trypsin digestion products. The intensity of the GTP-dependent band is expressed as a percent of the total intensity in the lane. Each point represents the mean of at least three experiments ± 2 × S.E.

erated nucleotide exchange rates (Fig. 5*B*), consistent with previous reports of mutagenesis at the Arg[144] position (4).

DISCUSSION

Analysis of Trypsin Digest Products of in Vitro Translated Gα_t to Evaluate Nucleotide Exchange Kinetics—Since Gα_t is refractory to expression in bacteria (24) and is cumbersome to express in insect cells (16), we chose to express Gα_t *in vitro* and analyze nucleotide exchange rates using trypsin digestion. The pattern of proteolytic fragments resulting from trypsin digestion directly reflects the conformation of Gα_t and, therefore, the identity of the bound nucleotide (25, 26). Trypsin proteolysis of expressed Gα_t yielded ~23-kDa fragments following incubation with GDP and ~34-kDa fragments following activation with either AlF$_4^-$ or GTPγS (Fig. 2). These observations are consistent with previously published results (23, 27).

Trypsin proteolysis of *in vitro* translated Gα_t allowed for the precise quantitation of basal and R*-catalyzed nucleotide exchange rates. By using both the ~23- and the ~34-kDa bands, the calculation of nucleotide exchange rates was internally normalized and took into consideration both the GDP- and the GTPγS-bound fractions. As a result, the data were very reproducible, and samples in which only a small fraction of the total expressed protein was functional could be analyzed. Additionally, the methodology was rapid enough to allow for the characterization of relatively large numbers of mutants in parallel.

The kinetic parameters for Gα_t activation derived from the trypsin digestion assay are consistent with data reported using other traditional methodologies (24, 28) as well as with analysis of retinal Gα_t studied with the fluorescence activation assay (Fig. 5). Additionally, analysis of the mutant A322S by trypsin proteolysis indicated that the basal rate of activation was >60-fold greater than that of wild-type Gα_t (not shown). This result is also in agreement with published data using different methodologies on the analogous mutation in Gα_s and in Gα_{i1} (21, 22).

Several control reactions demonstrated the fidelity of the R*-catalyzed assay. The rate of rhodopsin-dependent activation was sensitive to light (not shown), to the concentration of rhodopsin from 0–100 nM, and to the presence of added $G\beta\gamma_t$. A mutation near the carboxyl terminus of $G\alpha_t$ (G348P) that was previously reported to disrupt rhodopsin-transducin interactions (23) was not activated (not shown).

This expression and assay system offers additional flexibility not explored in the present work. Expressed recombinant rhodopsin could be used in place of retinal rhodopsin to test the combined effects of mutations of rhodopsin and transducin.[3] Other proteins (*e.g.* $G\beta\gamma_t$ mutants, regulator of G protein signaling proteins, etc.), could be co-translated with $G\alpha_t$ in the *in vitro* system (25). Furthermore, this system will likely prove useful in the kinetic characterization of other G protein subtypes, such as cone transducin, which are difficult to express heterologously.

Site-directed Mutation of Lys[273] or Lys[276] Increases Basal Nucleotide Exchange Rates—Replacement of Lys[276] or Lys[273] with alanine increased the basal rate of nucleotide exchange ~5-fold in $G\alpha_t$ (Fig. 3*D*, Table I). Replacement of the adjacent Lys[275], which in the crystal structure is oriented toward the solvent (Fig. 1), had no effect. Replacement of Lys[276] with a negatively charged glutamic acid increased basal nucleotide exchange rates more dramatically (~10-fold) than the neutral alanine replacement mutant. However, mutation to a positively charged arginine did not alter the activation rate. Together, these results suggest that the function of Lys[276] and Lys[273] is dependent on positive charge and orientation toward the interior of the protein. Interestingly, in the activated, GTPγS-bound structure of $G\alpha_t$, Lys[276] is rotated outward toward the solvent relative to the GDP-bound conformation (Fig. 1*B*). The K276A mutant may anticipate this active conformation.

Lys[276] and Lys[273] both lie in the third of four regions of $G\alpha_t$ for which there is no homologous sequence in the monomeric G protein Ras. The four regions are known as Insert 1 through Insert 4 (1). Specific functions have been attributed to Insert 1 (the helical domain), Insert 2 (the Switch III region), and Insert 4 (which may interact with heptahelical receptors). The present work is the first to identify a functional role for residues in Insert 3 of $G\alpha_t$.

The structure of GDP-bound $G\alpha_t$ reveals that Lys[276] and Lys[273] lie near to and possibly form ionic interactions with Asp[227]. This observation suggests that the reason for accelerated nucleotide exchange rates caused by mutations of Lys[276] and Lys[273] might involve disruption of interactions with Asp[227]. To test this hypothesis, the K276A and K273A mutations were combined with mutation of D227N to produce the K276A/D227N and K273A/D227N double mutants. If the effects of K276A were due solely to breaking of an interaction with Asp[227], then the Lys[276] mutation should not increase the rate of nucleotide exchange in the context of D227N or D227A mutants. Indeed, the increase in the basal rate of activation caused by the K276A and K273A mutations was reduced (from ~5-fold to ~2-fold relative to wild-type) when combined with D227N (Fig. 4). However, since the rate of the D227N mutant alone is 2-fold slower than that of wild-type, the effect of the K276A mutation is roughly the same (*i.e.* a ~5-fold increase in rate) whether introduced into a wild-type or a D227N background. Similar results were obtained with a D227A mutation. Thus, the origin of the increase in basal nucleotide exchange rates by the K276A and K273A mutation is not merely due to disruption of interactions with Asp[227].

Lys[276] also appears to interact across the interdomain interface with S140. Replacement of Ser[140] with alanine, which would have disrupted hydrogen bonding to K276A, did not affect the rate of activation. Thus, breaking of the putative Ser[140]-Lys[276] interaction does not fully explain the effects of the K276A mutation. There appear to be other unidentified requirements for positively charged side chains in the αG region to maintain low basal rates of nucleotide exchange.

Mutation of Asp[227] slows the rate of basal nucleotide exchange, both in the context of the wild-type protein as well as in the K276A mutant (Fig. 4). This is surprising since $G\alpha_t$ has an extremely low rate of basal nucleotide exchange, as is demanded by the low background noise required for sensitive light detection by photoreceptors. Other mutations in the Switch III regions also appear to slightly reduce the basal rate of nucleotide exchange, including M228L and V231A (Fig. 3; Table I). The origins of these effects, which are relatively small, are unclear. Previously, it has been demonstrated that the entire Switch III region can be deleted from $G\alpha_t$ without disrupting the ability to bind nucleotides (29). The rates of nucleotide exchange in these Switch III-deleted constructs were not characterized, but such studies might illuminate the role of Switch III in facilitating or impeding nucleotide exchange.

Interdomain Interactions in $G\alpha_t$ Do Not Affect Basal or Rhodopsin-catalyzed Nucleotide Exchange Rates—When the structure of $G\alpha_t$ was determined, the nucleotide was found to reside in a deep cleft between the Ras-like domain and the helical domain (1). It was proposed that rhodopsin might accelerate the nucleotide exchange rate by opening the cleft (1, 30). Similarly, interactions between these domains could control the rate of basal nucleotide exchange. $G\alpha_t$ has a very low rate of basal nucleotide exchange as compared with related G proteins and a very high rate of R*-catalyzed exchange. If interdomain interactions were important mediators of either of these processes, one might expect nucleotide exchange rates in $G\alpha_t$ to be particularly sensitive to mutation of residues involved in those interactions. However, none of the $G\alpha_t$ mutants characterized in this report significantly affected either basal or R*-catalyzed rates.

Close analyses of G protein structures indicate that opening of the interdomain cleft is not necessarily an energetic barrier to nucleotide release. The helical domain does not contribute many contacts to the nucleotide binding pocket, and certain monomeric G proteins, which do not have a helical domain at all, release GDP more slowly than some heterotrimeric G proteins subtypes (31). A crystal structure of the $G\alpha_{i1}$ mutant A326S, which releases GDP ~250-fold faster than wild-type $G\alpha_{i1}$, does not reveal any alteration in the interdomain interactions, suggesting that an open cleft is not a prerequisite of fast nucleotide exchange (21). In addition, the reported increases in nucleotide release rates resulting from mutations at the interdomain interface of $G\alpha_{i1}$ and $G\alpha_s$ are relatively modest (~5–10-fold) as compared with mutations in other regions of G proteins hypothesized to be involved in regulating nucleotide exchange rates. For example, we observed >150-fold increases in nucleotide exchange rates in mutations of certain residues of the α5-helix of $G\alpha_t$, a structure implicated in the mechanism of rhodopsin-catalyzed activation (34). In summary, the opening of the interdomain cleft may not necessarily be a rate-determining step in nucleotide exchange in G proteins.

The Function of Residues at the Interdomain Interface Differs among $G\alpha_t$, $G\alpha_{i1}$, and $G\alpha_s$—Many of the residues mutated in this study, such as Ser[140], Gln[143], Met[228], and Val[231], have been previously found to alter basal or receptor-catalyzed nucleotide exchange rates in the related G proteins, $G\alpha_s$ and $G\alpha_{i1}$. In $G\alpha_s$, a mutation in the Switch III region, R258W (corre-

---

sponding to Val[231] in $G\alpha_t$), was found in a patient with Albright's hereditary osteodystrophy (5). Biochemical studies indicated that replacement of Arg[258] to tryptophan and to alanine, as well as alteration of a proposed interacting residue, Gln[170] of the helical domain (corresponding to Gln[143] in $G\alpha_t$), led to increases in the basal nucleotide exchange rate (5, 6). These mutations were hypothesized to widen the interdomain cleft. Other studies in $G\alpha_s$ found that mutation of Arg[258] or Asn[167] (corresponding to Ser[140] in $G\alpha_t$) disrupted receptor-catalyzed activation (8), suggesting that the receptor induces structural changes that are communicated across the interdomain interface. In $G\alpha_{i1}$, mutation of either Leu[232] or Arg[144] (corresponding to Met[228] and Ser[140], respectively, in $G\alpha_t$) increased the basal nucleotide exchange rate by disrupting a proposed interdomain hydrophobic interaction (4). The effects of mutating Arg[144] were corroborated by the results of the R144S mutant in the current work (Fig. 5*B*).

The residues analogous to those proposed to interact with each other across the interdomain interface in $G\alpha_s$ and $G\alpha_{i1}$ are also potentially interacting in $G\alpha_t$ (Fig. 1*B*). In many cases, however, the amino acids are not conserved. For example, Val[231] and Gln[143] of $G\alpha_t$, which correspond to the proposed interaction between Arg[258] and Gln[170] in $G\alpha_s$, are adjacent. Ser[140] and Met[228] (corresponding to Arg[144] and Leu[232] of $G\alpha_{i1}$) and Ser[140] and Asp[227] (corresponding to the proposed interaction of Asn[167] and Asn[254] of $G\alpha_s$ (8)) are similarly adjacent. However, in contrast to the results with $G\alpha_{i1}$ and $G\alpha_s$, replacement of these residues in $G\alpha_t$ did not affect nucleotide exchange rates. These results suggest that the interdomain interface residues are functionally different in $G\alpha_t$ than in $G\alpha_{i1}$ and $G\alpha_s$. Counterintuitively, $G\alpha_{i1}$ and $G\alpha_s$, which exchange nucleotides faster than $G\alpha_t$, appear to have tighter and more sensitive interactions across the interdomain interface than those of $G\alpha_t$.

Both Lys[273] and Lys[276] of $G\alpha_t$ are conserved in $G\alpha_{i1}$. However, the structure of GDP-bound $G\alpha_{i1}$ reveals that Lys[280] (cognate to Lys[276] of $G\alpha_t$) is oriented toward the solvent instead of toward the Switch III region as in $G\alpha_t$ (Fig. 1*C*). Functionally, mutation of Lys[280] and Lys[277] to alanine did not lead to increases in nucleotide exchange rates in $G\alpha_{i1}$, as was observed in $G\alpha_t$. Thus, conserved residues, Lys[276] and Lys[273] of $G\alpha_t$, are found to serve different roles and to assume different structures in closely related G proteins.

In conclusion, the data in this report ascribe a role to Lys[273] and Lys[276] in the αG region of $G\alpha_t$ in maintaining low basal rates of nucleotide exchange. However, unlike in $G\alpha_{i1}$ and $G\alpha_s$,

interactions that span the interdomain interface do not appear to be important in regulating either basal or rhodopsin-catalyzed nucleotide exchange rates. Differences exist in the organization of the interdomain interface among $G\alpha_t$, $G\alpha_{i1}$, and $G\alpha_s$, and even between conserved residues in $G\alpha_{i1}$ and $G\alpha_t$.

REFERENCES

1. Noel, J. P., Hamm, H. E., and Sigler, P. B. (1993) *Nature* **366**, 654–663
2. Iiri, T., Farfel, Z., and Bourne, H. R. (1998) *Nature* **394**, 35–38
3. Mixon, M. B., Lee, E., Coleman, D. E., Berghuis, A. M., Gilman, A. G., and Sprang, S. R. (1995) *Science* **20**, 954–960
4. Remmers, A. E., Engel, C., Liu, M., and Neubig, R. R. (1999) *Biochemistry* **38**, 13795–13800
5. Warner, D. R., Weng, G., Yu, S., Matalon, R., and Weinstein, L. S. (1998) *J. Biol. Chem.* **273**, 23976–23983
6. Warner, D. R., and Weinstein, L. S. (1999) *Proc. Natl. Acad. Sci. U. S. A.* **96**, 4268–4272
7. Marsh, S. R., Grishina, G., Wilson, P. T., and Berlot, C. H. (1998) *Mol. Pharmacol.* **53**, 981–990
8. Grishina, G., and Berlot, C. H. (1998) *J. Biol. Chem.* **273**, 15053–15060
9. Sakmar, T. P., and Khorana, H. G. (1988) *Nucleic Acids Res.* **16**, 6361–6372
10. Garcia, P. D., Onrust, R., Bell, S. M., Sakmar, T. P., and Bourne, H. R. (1995) *EMBO J.* **14**, 4460–4469
11. Kuhn, H. (1980) *Nature* **283**, 587–589
12. Fung, B. K., Hurley, J. B., and Stryer, L. (1981) *Proc. Natl. Acad. Sci. U. S. A.* **78**, 152–156
13. Marin, E. P., Krishna, A. G., Zvyaga, T. A., Isele, J., Siebert, F., and Sakmar, T. P. (2000) *J. Biol. Chem.* **275**, 1930–1936
14. Fahmy, K., and Sakmar, T. P. (1993) *Biochemistry* **32**, 7229–7236
15. Kazmi, M. A., Snyder, L. A., Cypess, A. M., Graber, S. G., and Sakmar, T. P. (2000) *Biochemistry* **39**, 3734–3744
16. Min, K. C., Gravina, S. A., and Sakmar, T. P. (2000) *Protein Expression Purif.* **20**, 514–526
17. Faurobert, E., Otto-Bruc, A., Chardin, P., and Chabre, M. (1993) *EMBO J.* **12**, 4191–4198
18. Lambright, D. G., Noel, J. P., Hamm, H. E., and Sigler, P. B. (1994) *Nature* **369**, 621–628
19. Sondek, J., Lambright, D. G., Noel, J. P., Hamm, H. E., and Sigler, P. B. (1994) *Nature* **372**, 276–279
20. Mazzoni, M. R., Malinski, J. A., and Hamm, H. E. (1991) *J. Biol. Chem.* **266**, 14072–14081
21. Posner, B. A., Mixon, M. B., Wall, M. A., Sprang, S. R., and Gilman, A. G. (1998) *J. Biol. Chem.* **273**, 21752–21758
22. Iiri, T., Herzmark, P., Nakamoto, J. M., van Dop, C., and Bourne, H. R. (1994) *Nature* **371**, 164–168
23. Osawa, S., and Weiss, E. R. (1995) *J. Biol. Chem.* **270**, 31052–31058
24. Skiba, N. P., Bae, H., and Hamm, H. E. (1996) *J. Biol. Chem.* **271**, 413–424
25. Neer, E. J., Denker, B. M., Thomas, T. C., and Schmidt, C. J. (1994) *Methods Enzymol.* **237**, 226–239
26. Fung, B. K., and Nash, C. R. (1983) *J. Biol. Chem.* **258**, 10503–10510
27. Mazzoni, M. R., and Hamm, H. E. (1996) *J. Biol. Chem.* **271**, 30034–30040
28. Ramdas, L., Disher, R. M., and Wensel, T. G. (1991) *Biochemistry* **30**, 11637–11645
29. Li, Q., and Cerione, R. A. (1997) *J. Biol. Chem.* **272**, 21673–21676
30. Bourne, H. R. (1993) *Nature* **366**, 628–629
31. Sprang, S. R. (1997) *Annu. Rev. Biochem.* **66**, 639–678
32. Kraulis, P. J. (1991) *J. Appl. Crystallogr.* **24**, 946–950
33. Merritt, E. A., and Bacon, D. J. *Methods Enzymol.* **277**, 505–524
34. Marin, E. P., Krishna, A. G., and Sakmar, T. P. (2001) *J. Biol. Chem.* **276**, in press